Biomedical Signal Processing and Control 65 (2021) 102326

Contents lists available at ScienceDirect

Biomedical Signal Processing and Control

journal homepage: www.elsevier.com/locate/bspc

A new automated CNN deep learning approach for identification of ECG congestive heart failure and arrhythmia using constant-Q non-stationary Gabor transform

Ahmed S. Eltrass *, Mazhar B. Tayel, Abeer I. Ammar

Electrical Engineering Department, Faculty of Engineering, Alexandria University, Alexandria, Egypt

ARTICLE INFO

Keywords:
Deep learning (DL)
Convolutional neural network (CNN)
Electrocardiogram (ECG)
Arrhythmia (ARR)
Congestive heart failure (CHF)
Normal sinus rhythm (NSR)

ABSTRACT

Electrocardiogram (ECG) is an important noninvasive diagnostic method for interpretation and identification of various kinds of heart diseases. In this work, a new Deep Learning (DL) approach is proposed for automated identification of Congestive Heart Failure (CHF) and Arrhythmia (ARR) with high accuracy and low computational requirements. This study introduces, for the first time, a new ECG diagnosis algorithm that combines Convolutional Neural Network (CNN) with the Constant-Q Non-Stationary Gabor Transform (CQ-NSGT). The CQ-NSGT algorithm is investigated to transform the 1-D ECG signal into 2-D time-frequency representation that will be fed to a pre-trained CNN model, called AlexNet. Extracted features with the AlexNet architecture are used as relevant features to be discriminated by a Multi-Layer Perceptron (MLP) technique into three different cases, namely CHF, ARR, and Normal Sinus Rhythm (NSR). The performance of the proposed CNN with CQ-NSGT is compared versus CNN with Continuous Wavelet Transform (CWT), revealing the effectiveness of the CQ-NSGT algorithm. The proposed approach is examined with real ECG records, and the experimental results show the superior performance of the proposed approach over other existing techniques in terms of accuracy 98.82%, sensitivity 98.87%, specificity 99.21%, and precision 99.20%. This demonstrates the effectiveness of the proposed system in enhancing the ECG diagnosis accuracy.

1. Introduction

The Electrocardiogram (ECG) is a diagnostic method that measures and records the electrical activity of the heart muscles. ECG is widely used in several medical studies for interpretation and identification of heart disorders. One of these disorders is Congestive Heart Failure (CHF), which is a serious cardiac condition associated with high mortality and morbidity rates. In CHF, the heart cannot pump blood efficiently to supply organs with oxygen and nutrients, causing easy fatigue, breathlessness, and generalized swelling. According to the European Society of Cardiology (ESC), at least 26 million adults are diagnosed with CHF worldwide, while 3.6 million are newly diagnosed every year [1]. 17–45% of patients diagnosed with CHF die within the first year and the rest within 5 years [1]. However, successful early diagnosis of CHF can enhance the treatment options and reduce the death rates. Another serious disorder caused by irregular heart rate is Arrhythmia (ARR), which is most often responsible for sudden deaths. ARRs can be classified into two main classes: ventricular and supraventricular. Ventricular ARRs occur in the lower chambers of the heart, called ventricles, while supraventricular ARRs originate from above the ventricles, usually in the top chambers of the heart, called the atria. Both classes are investigated in the current study.

ECG Diagnosis of ARR and CHF requires accurate and uniform evaluation by experienced cardiologists, which is tedious and time consuming. Therefore, it is very important to develop new efficient Computed Aided Diagnosis (CAD) systems that can enhance the diagnostic reliability of ECG recordings. With the advances of signal processing and Machine Learning (ML) techniques, several CAD systems were developed over the last decades for automated identification of heart diseases [2–4]. Deep learning (DL) represents the most modern and effective branch of ML in biomedical engineering applications which utilizes a hierarchical level of Neural Network (NN) [5,6]. There are several DL architectures such as Stacked Auto-Encoder (SAE), Deep Belief Networks (DBNs), and Convolutional Neural Networks (CNNs) [7, 8]. One of the most effective architectures in image processing applications is the deep CNN, the focus point of this work.

* Corresponding author.
E-mail address: ahmed.eltrass@alexu.edu.eg (A.S. Eltrass).

https://doi.org/10.1016/j.bspc.2020.102326
Received 21 March 2020; Received in revised form 27 September 2020; Accepted 1 November 2020
Available online 8 December 2020

Several studies investigated different ML techniques for distinguishing patients with CHF from Normal Sinus Rhythm (NSR) subjects [9–17]. Most of these studies employed classifiers with relatively simple structures such as Support Vector Machine (SVM) and K-Nearest Neighbor (KNN), and they were trained on a group of hand-crafted features extracted from HRV records. In [11], the Renyi entropy exponents of ECG are extracted and combined with the standard time domain features for CHF diagnosis, and the results showed an accuracy of 87.9%. In [14], the CHF is diagnosed using HRV analysis by extracting the fuzzy and permutation entropies at distinct frequency scales and employing Bhattacharyya ranking method for feature selection, achieving an accuracy of 98.21%. In [15], a comparison between time-domain, frequency-domain, and non-linear dynamics features was investigated for distinguishing CHF patients from NSR subjects using SVM classifier with an accuracy of 90.95%. The same HRV features were also investigated in [16], and the best time scale was employed to diagnose CHF with an accuracy of 94.4%. A multi-stage system consisting of perceptron classifiers that are trained by a genetic algorithm in the first two stages, and a binary classifier in the third stage was developed in [17] to diagnose CHF with an accuracy of 98.8%.

All previous feature-based ML techniques require high computational time to select the most important ECG features which may vary for different datasets. Also, the classification performance is mainly dependent on the feature selection process. To overcome these drawbacks, DL techniques [18–22] have been recently employed for ECG diagnosis. Note that training a deep CNN from scratch is difficult and time consuming because it requires huge amount of training data. On contrast, training a deep CNN with small amount of data may lead to over-fitting problems [23]. Transfer learning represents a versatile solution to overcome these difficulties. It allows leveraging of existing NNs that have been trained on large data sets to transfer the knowledge to another classification task without the need of large training data [24]. Several pre-trained CNNs, including AlexNet [25], VGGNet [26], and GoogleNet [27] were trained on the ImageNet Large Scale Visual Recognition Challenge (ILSVRC) dataset. Several pre-trained CNNs achieved high classification performance in medical imaging applications [28–31].

Most of recent ECG diagnosis systems based on DL techniques [32–35] achieve reasonable results of distinguishing CHF patients from NSR with accuracies up to 98%. However, it is still very challenging to develop an accurate fully automated diagnosis system for ECG multi-class classification. The aim of this work is to propose a new ECG diagnosis system based on combining a pre-trained CNN model, AlexNet, with the Constant-Q Non-Stationary Gabor Transform (CQ-NSGT) for not only distinguishing patients with CHF from NSR subjects but also from ARR subjects with high accuracy and low computational cost. The remaining parts of this paper are structured as follows. Section II presents the methodology and the CQ-NSGT algorithm, followed by the architecture of the pre-trained CNN, AlexNet. Section III shows the experimental results of the proposed approach in terms of diagnosis accuracy, specificity, sensitivity, and precision using real ECG records. In Section IV, the results are discussed and compared with other recent ECG diagnosis systems.

2. Methodology

The proposed diagnosis CAD system consists of three stages: ECG data pre-processing and segmentation, feature extraction, and classification. Fig. 1 illustrates the structure of the proposed approach. In order to investigate the usefulness of the proposed system, clinical ECG signals for the three subjects (ARR, CHF, and NSR) taken from three databases, namely Massachusetts Institute of Technology–Beth Israel Deaconess Medical Center (MIT-BIH) ARR database [36,37], MIT-BIH Normal Sinus Rhythm (NSR) [36], and BIDMC Congestive Heart Failure (CHF) [36,38] are investigated. According to Association for the Advancement of Medical Instrumentation (AAMI) standard, the MIT-BIH ARR database is the most representative open access database for ARR, and it is the most utilized and recommended database for ARR detection. It contains a wide variety of ARR waveforms, including complex ventricular, junctional, supraventricular, and conduction abnormalities. There are 96 ECG records in the MIT-BIH ARR database, 30 ECG records in the BIDMC CHF database, and 36 ECG records in the MIT-BIH NSR database, yielding a total number of 162 ECG signals. The 162 ECG records of lead II and VI were carefully reviewed and labeled by multiple cardiologists. In the current study, all the 162 ECG signals are investigated to avoid any selectivity of the cases under investigation which authenticates the results of the proposed approach and validates the comparison with other existing techniques.

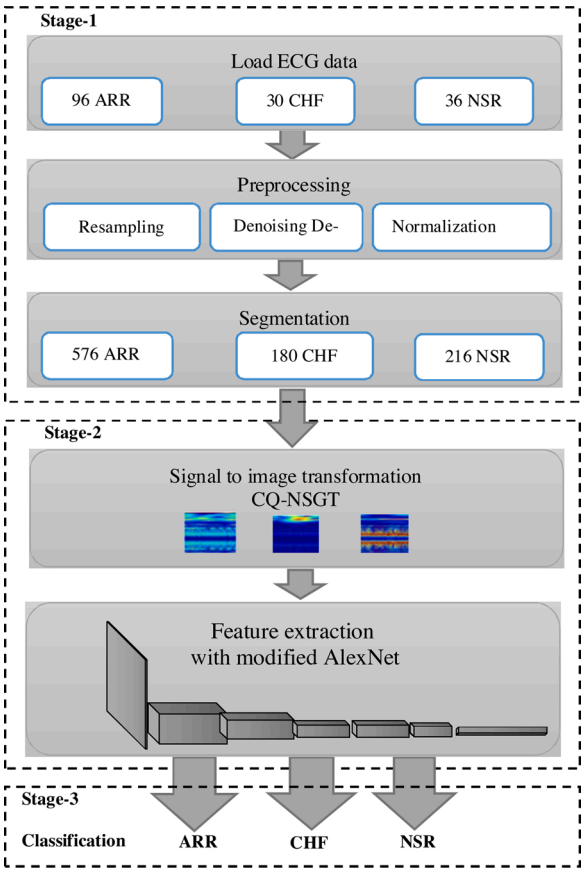

Fig. 1. The structure of the proposed approach.

2.1. ECG data acquisition and preprocessing

First, all ECG records are resampled to a common sampling rate of 128 Hz to establish uniformity and standardization for all data investigated in the current work. Also, all ECG data are normalized to remove the offset effect and to standardize the ECG signal amplitude. Note that ECG signals are usually corrupted with several unwanted noise and artifact sources, which lead to poor signal quality and wrong diagnosis of heart diseases. The most common artifacts are the Power Line Interference (PLI), the Baseline Wonder (BW), and the ElectroMyoGraphy (EMG) [39]. In the current study, a multi-stage kernel adaptive filter design [40] is used to eliminate all unwanted noise and artifact sources from the input ECG signal, while preserving its important and tiny features.

After removing noise and artifact sources from the 162 ECG records, each denoised ECG signal is divided into 6 segments each with a specific length of 10,000 samples (78 s). This means that 972 ECG segments are used for training and testing using k-fold cross-validation technique [41]. Fig. 2 shows three ECG segments each of length 8 s for the three

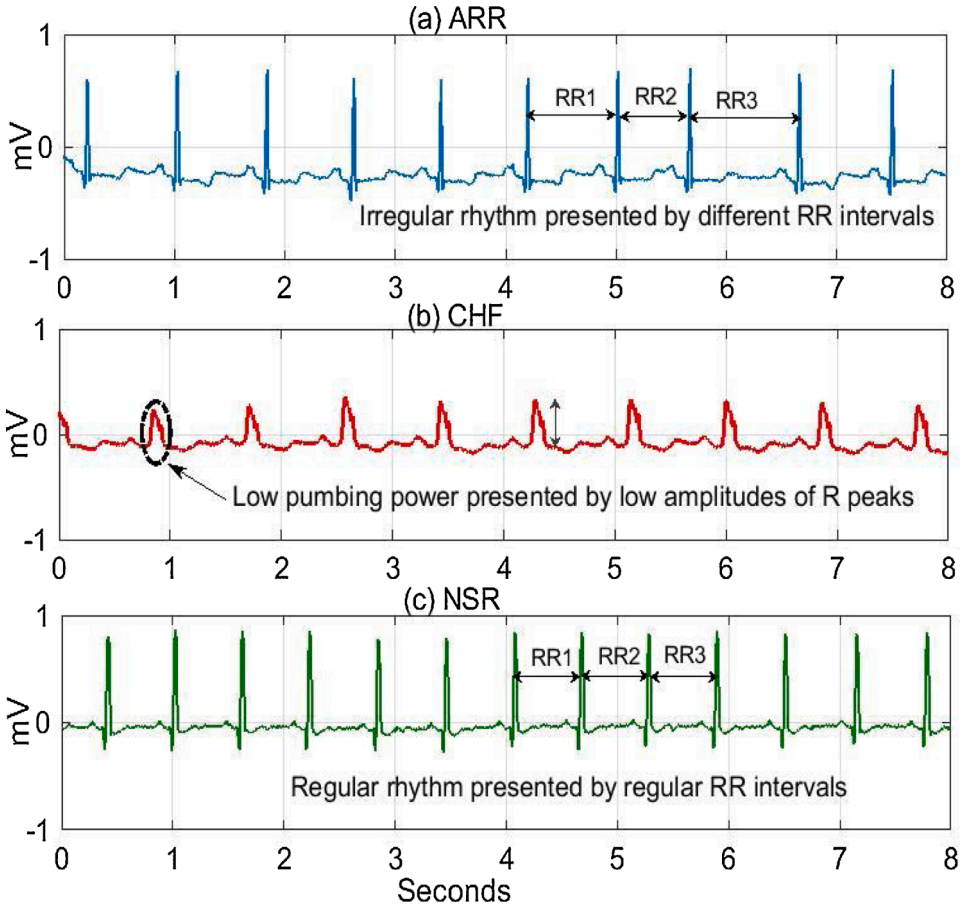

Fig. 2. Three ECG records each of length 8 s for three cases: (a) ARR; (b) CHF; and (c) NSR.

cases of ARR, CHF, and NSR. Fig. 2a illustrates the irregular HRV with different RR intervals for ARR case compared to the regular rhythm in the NSR example shown in Fig. 2c. It can be noted from Fig. 2b that the weakness of pumping power caused by CHF is represented by the low amplitudes of R-peaks compared to the NSR case of Fig. 2c.

2.2. ECG signal to image transformation with CQ-NSGT

Since any CNN architecture requires 2-D input images, the pre-processed 1-D ECG data should be transformed efficiently into 2-D image. Traditional signal transformations such as Short-Time Fourier transform (STFT) and Continuous Wavelet Transform (CWT) were investigated for ECG analysis [42–45]. The STFT imposes a regular spacing of frequency bins, causing a constant frequency resolution over the whole frequency range.

The fixed frequency resolution of STFT is not optimal for the analysis of non-stationary signals like ECG. Due to the non-stationary nature of ECG signals, the time-frequency representation with variable frequency resolution is very important for perfect track of dynamic changes and frequency variations over time within the ECG signal, and hence achieving accurate ECG classification. The CWT provides variable time-frequency resolution, but it requires high computational time. Therefore, an efficient signal transformation algorithm with variable frequency resolution is needed to track the non-stationarity of ECG signal and extract its important features, while requiring low computational time.

The Constant-Q Transform (CQT), originally proposed by [46], provides geometric non-linear spacing of the frequency bins, allowing a variable frequency resolution depending on the center frequencies of windows used for each bin. The ratio of the center frequency to bandwidth, called the Q factor, is constant over all bins, and thus the frequency resolution is better for low frequencies, whereas time resolution increases with frequency increase. However, the original CQT is non-invertible. To overcome this drawback, the Non-Stationary Gabor Transform (NSGT) is employed in the implementation of CQT, allowing for perfect reconstruction with low computational cost. The invertible CQT is called constant-Q Non-Stationary Gabor Transform (CQ-NSGT) [47,48]. In standard Gabor analysis, a fixed size window tiles the time-frequency plane [49]. The nonstationary Gabor frame employs various windowing functions with different sizes to tile the time-frequency plane, allowing for more flexibility in signal representation. The CQ-NSGT algorithm has the ability to overcome the main problems of classical implementations of constant-Q transforms, in particular, lack of invertibility and high computational requirements. Also, the variable frequency resolution of the CQ-NSGT is well suited to the analysis and classification of the non-stationary ECG signals containing short and high-frequency components.

In this work, the CQ-NSGT algorithm is investigated, for the first time, to capture the change in the ECG power and convert it into 2-D image. The input ECG signal f can be represented as a sum of atoms $\varphi_{n,k}$, weighted by coefficients $c_{n,k}$ as follows [48]:

$$f = \sum_{n,k} c_{n,k}\varphi_{n,k} \tag{1}$$

where the indexes (n,k) represent each atom location and concentration in time and frequency. Frame theory determines the conditions for the existence of expansion (1) and the required coefficients leading to stable and perfect reconstruction.

Considering frames for $\mathbb{C}^L$, i.e. vector spaces of finite and discrete signals, assume a collection of atoms $\varphi_{n,k} \in \mathbb{C}^L$ with $(n,k) \in I_N \times I_K$ for

finite index sets I_N and I_K. The frame operator S can be defined as:

$$Sf = \sum_{n,k} \langle f, \varphi_{n,k} \rangle \varphi_{n,k} \tag{2}$$

where $\langle f, \varphi_{n,k} \rangle$ is the inner product of f and $\varphi_{n,k}$. If the set of functions $\{\varphi_{n,k}\}_{(n,k)\in I_N \times I_K}$ represents an orthonormal basis, then S represents an identity operator. For all $f \in \mathbb{C}^L$, with invertible S on $\mathbb{C}^L$, the set of functions $\{\varphi_{n,k}\}_{(n,k)\in I_N \times I_K}$ is considered as a frame. In this case, the dual frame $\widetilde{\varphi_{n,k}}$ can be defined as:

$$\widetilde{\varphi_{n,k}} = S^{-1}\varphi_{n,k} \tag{3}$$

Reconstructing f from the coefficients $c_{n,k}$ is possible and can be obtained by substituting from (2) and (3) into (1) as follows:

$$\begin{aligned} f &= S^{-1}Sf = \sum_{n,k} \langle f, \varphi_{n,k} \rangle S^{-1}\varphi_{n,k} = \sum_{n,k} c_{n,k}\widetilde{\varphi_{n,k}} = SS^{-1}f \\ &= \sum_{n,k} \langle f, S^{-1}\varphi_{n,k} \rangle \varphi_{n,k} = \sum_{n,k} \langle f, \widetilde{\varphi_{n,k}} \rangle \varphi_{n,k} \end{aligned} \tag{4}$$

The construction of CQ-NSGT algorithm relies on the following parameters: minimum and maximum frequencies ξ_{min} and ξ_{max} (in Hz), respectively, the number of frequency bins per octave B, and the sampling frequency ξ_s (in Hz). In CQ-NSGT, band-limited window functions $\varphi_k \in \mathbb{C}^L$ with center frequencies ξ_k are considered. Like the classical CQT [46], ξ_k should satisfy the following condition [47,48]:

$$\xi_k = \xi_{min} 2^{\frac{k-1}{B}},\ k = 1, 2, \ldots K \tag{5}$$

where K is an integer such that $\xi_{max} < \xi_k < \xi_s/2$, and $\xi_s\ /2$ is the Nyquist frequency. Note that the maximum frequency ξ_{max} is limited to be less than the Nyquist frequency $\xi_s\ /2$.

The bandwidth Ω_k of φ_k, which represents the support of the window in frequency, is set to be $\Omega_k = \xi_{k+1} - \xi_k$, for $k = 1, 2, \ldots K-1$, which leads to a constant Q-factor given by $Q = \xi_k/\Omega_k = \left(2^{\frac{1}{B}} - 2^{\frac{-1}{B}}\right)^{-1}$. In order to keep the same Q-factor for all relevant frequency bins, the band width Ω_k should have the following values [47]:

$$\Omega_k = \begin{cases} 2\xi_{min},\ k = 0 \\ \xi_k/Q,\ k = 1, \ldots, K \\ \xi_s - 2\xi_K,\ k = K+1 \\ \xi_{2K+2-k}/Q,\ k = K+2, \ldots, 2K+1. \end{cases} \tag{6}$$

The choice of window function φ_k satisfying the frame conditions is very important. In this work, a standard Hann window $\widehat{h}$ centered at 0 with unit support length is employed. Note that Fourier transforms of band-limited windows φ_k, well-localized in time $\widehat{\varphi}_k = \mathscr{F}\varphi_k$ are centered around possibly geometrically spaced frequency points ξ_k. The atoms φ_k can be obtained by translation and dilation of $\widehat{h}$ as follows [47]:

$$\widehat{\varphi_k}[j] = \widehat{h}((j\xi_s/L - \xi_k)/\Omega_k) \tag{7}$$

where $k = 1, \ldots K, K+2, \ldots, 2K+1$ and $j = 0, \ldots, L-1$. For the windows of the 0 and Nyquist frequencies, a plateau-like function $\widehat{g}$ is utilized. The values of φ_0 and φ_{k+1} are obtained by setting $\widehat{\varphi_k}[j] = \widehat{\psi}\ ((j\xi_s/L - \xi_k)/\Omega_k), k = 0, K+1$.

Assume that T_x is a time shift by x, M_ω is a frequency shift by ω, and $\widehat{f} = \mathscr{F}f$ is the Fourier transform of f. The frequency dependent time-shift parameters a_k are chosen based on the following condition:

$$a_k \le \frac{1}{|\mathfrak{T}_k|} \text{ for all } k \tag{8}$$

where $|\mathfrak{T}_k|$ is the interval length which contains the support of $\widehat{\varphi_k}$. The frame members can be determined by setting $\varphi_{n,k} = T_{na_k}\varphi_k$.

For the collection of time-shift (hop-sizes) a_k of the constructed windows, the condition $a_k < \xi_k/\Omega_k$ should be satisfied. Then, the frame members $\varphi_{n,k}$ can be obtained by their Fourier transforms as follows:

$$\widehat{\varphi_{n,k}} = M_{-na_k}\widehat{\varphi_k},\ n = 0, \ldots, \lfloor \frac{L}{a_k} \rfloor - 1, \tag{9}$$

It can be concluded that the CQ-NSGT approach guarantees perfect regeneration of the signal f from the coefficients $c_{n,k}$ as follows:

$$f = \sum_{k=0}^{2K+1} \sum_{n=0}^{\lfloor \frac{L}{a_k} \rfloor - 1} c_{n,k}\widetilde{\varphi_{n,k}} \tag{10}$$

The CQ-NSGT algorithm is employed to transform the input 1-D ECG signal into 2-D time-frequency representation for three cases of ARR, CHF, and NSR. Fig. 3 shows the 2-D time-frequency image for three ECG segments of ARR, CHF, and NSR subjects. The shown images of Fig. 3 represent the signal strength over time at different frequencies. The vertical and horizontal axes represent the frequency and time, respectively, while the normalized amplitude of a particular frequency at a specific time is represented by the color bar, which reveals the difference between the three cases. Fig. 3b shows the low pumping power over most of the frequency range for the CHF case, while Fig. 3a illustrates the irregular HRV for the ARR case. Fig. 3c shows the regular change in both frequency and time for the NSR subject.

2.3. Feature extraction and classification with CNN

A pre-trained deep CNN structure, AlexNet, is employed in the current work to extract the ECG features automatically, instead of training a deep CNN from scratch. Note that there are many other CNN architectures such as VGG-16, VGG-19, ResNet-50, ResNet-101, Inception-v3, and DenseNet, and we examined all of them and compared their performance with the AlexNET architecture. The AlexNET architecture outperformed all of these models and achieved the highest performance with the lowest computational time. The AlexNet architecture was trained on 1.2 million high-resolution RGB images from the ILSVRC dataset and it can be used to classify those images into 1000 different categories [25]. The CNN structure consists of two main parts. The first part is the automatic feature extraction of the input data, and the second part is the fully connected Multi-Layer Perceptron (MLP) which carries out the classification task.

The AlexNet architecture contains five convolutional layers, three pooling layers, two fully connected layers, and one output layer. The graphical representation of the proposed AlexNet CNN architecture is shown in Fig. 4, while the detailed layers information is shown in Table 1. As mentioned before, the invertible CQ-NSGT algorithm is investigated to transform the 1-D ECG signal into 2-D RGB image, which represents the input to the AlexNet architecture. In the first layer, the RGB image with size 227 × 227 × 3 passes through a convolutional layer with 96 feature maps of filter size 11 × 11 and a stride of 4 (the amount by which the filter shifts), which changes the image dimensions to be 55 × 55 × 96. Then, a max pooling layer with filter size 3 × 3 and a stride of 2 is used to reduce the image dimension to 27 × 27 × 96, while preserving the important characteristics of the input ECG signal. The second layer is same as the first layer but with 256 feature maps of size 5 × 5 and a stride of 1, resulting in an output of size 13 × 13 × 256. The third, fourth, and fifth layers are convolutional layers with filter size 3 × 3 and a stride of 1. The three fully connected layers are followed by a maximum pooling layer with 256 feature maps of filter size 3 × 3 and a stride of 2. The output of these layers is flattened through a fully connected layer with 9216 feature maps each of size 1 × 1 in the sixth layer. Next, there are other two fully connected layers with 4096 units. Each of the convolution layers uses the Rectified Linear Unit (ReLU) as an activation function. Finally, there is a soft-max output layer that calculates the probability of each class over the possible classes to provide

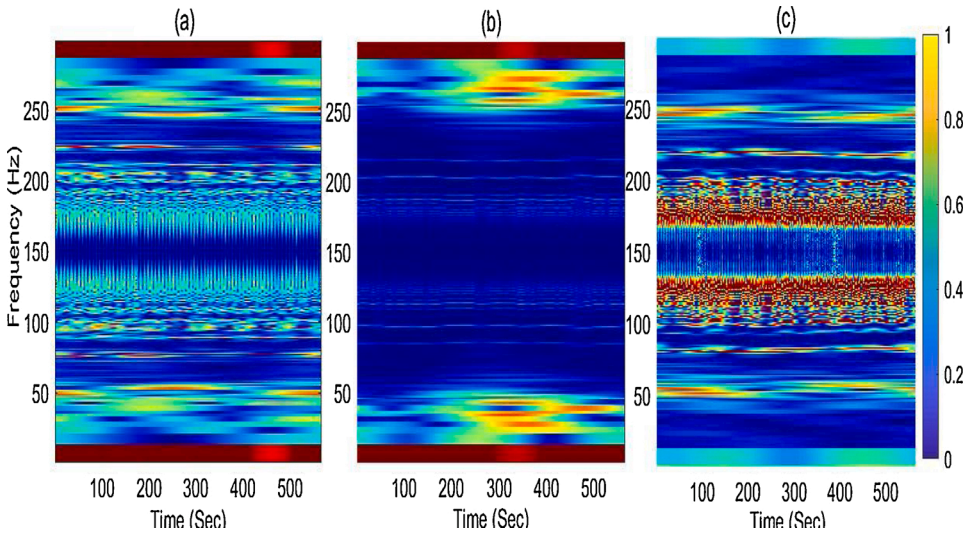

Fig. 3. The CQ-NSGT time-frequency representations of three different ECG segments for the cases: (a) ARR; (b) CHF; and (c) NSR.

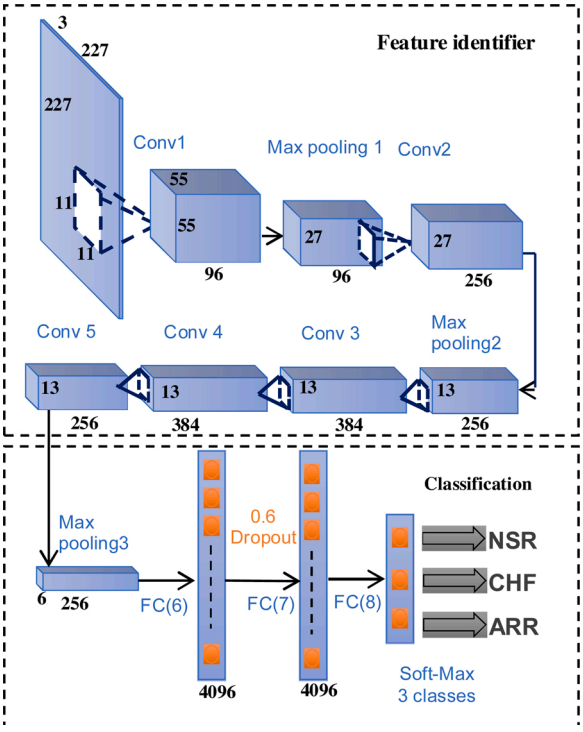

Fig. 4. The AlexNet architecture for the proposed approach.

the final decision [25]. In comparing with other CNN architectures, AlexNet has the following advantages: (i) The overfitting problem is reduced by using a dropout layer after the fully-connected layer; (ii) Max-pooling layers are utilized to enhance the richness of features; (iii) The ReLU function is utilized to speed up the training process and solve the problem of gradient explosion.

Training the AlexNet architecture is an iterative process which involves minimizing a loss function with the gradient descent algorithm. The gradient of the loss function is evaluated, and the weights of the gradient descent algorithm are updated in each iteration. Training can be tuned by setting several parameters such as initial learning rate, batch size, and maximum number of epochs. Initial learning rate is the initial step size in the direction of the negative gradient of the loss function. Batch size specifies how large a subset can be chosen from the training data to be used in each iteration. Maximum number of epochs specifies the number of epochs used for the training process, where one epoch is a full pass of the training algorithm over the entire dataset. Choosing the number of epochs is an important task because decreasing the number of epochs leads to under-fitting problems, while increasing the number of epochs results in over-fitting. These parameters are optimized to achieve the highest accuracy. In this work, a batch size of 15, maximum number of epochs of 20, and learning rate of 0.0001 are the optimum values for achieving the best classification results. Note that the AlexNet architecture reduces the over-fitting problems using two different methods: data augmentation and dropout. In the dropout process, a neuron is dropped from the network with a probability 0.5, which allows the network to be less sensitive to the specific weights of neurons and prevent complex co-adaptations on the training data [25]. In this study, the fully connected layers are modified to have the same size of the classes for the ECG classification (3 classes: ARR, CHF, and NSR). Also, the default 0.5 dropout probability is modified to be 0.6 for achieving robust performance.

The ECG multiclass classification is performed as follows. After ECG preprocessing and signal to image transformation processes, part of the resulted images $T_r = \{\mathrm{I}_i, y_i\}_{i=1}^{r}$ is used to train the AlexNet architecture, where I_i is the input image, r is the number of training samples, $y_i \in \{1, .., G\}$ is the corresponding class label of I_i, and G is the number of classes. The other part of resulted images $T_s = \{\mathrm{I}_j\}_{j=r+1}^{r+m}$ is used to test the AlexNet architecture, where m is the number of test samples. Each image I_i is fed to the AlexNet, and the resulted CNN feature representation, Z_i, can be expressed as [50]:

$$\mathbf{Z}_i = f^{CNN}(\mathrm{I}_i), i = 1, 2, .., r \tag{11}$$

where f^{CNN} represents the AlexNet layers. Those CNN features are the input to the last part of the network which consists of a hidden layer and a softmax regression layer. The hidden layer receives the feature input $\mathbf{Z}_i$ and maps it into another representation $\boldsymbol{h}_i^{(1)}$ of dimension $D^{(1)}$ through a nonlinear sigmoid activation function $u(\nu) = 1/(1 + \exp(-\nu))$ as follows:

$$\boldsymbol{h}_i^{(1)} = u(\boldsymbol{W}^{(1)}\mathrm{Z}_i + \boldsymbol{b}^{(1)}) \tag{12}$$

where $\boldsymbol{W}^{(1)}$ is the mapping weight matrix and $\boldsymbol{b}^{(1)}$ is the mapping bias vector. The softmax regression layer receives the resulted hidden representation $\boldsymbol{h}_i^{(1)}$ in order to perform the multiclass classification and produce an estimate probability for each class label $g = 1, 2, ..G$ as

Table 1
Summary of the CNN layers for the proposed AlexNet architecture.

Layer No	Type	Feature Map	Size	Kernel/Stride	Activation
	Input	1	227 × 227 × 3	–	–
1	Convolution	96	55 × 55 × 96	11 × 11/4	Relu
	MaxPooling	96	27 × 27 × 96	3 × 3/2	Relu
2	Convolution	256	27 × 27 × 256	5 × 5/1	Relu
	MaxPooling	256	13 × 13 × 256	3 × 3/2	Relu
3	Convolution	384	13 × 13 × 384	3 × 3/1	Relu
4	Convolution	384	13 × 13 × 384	3 × 3/1	Relu
5	Convolution	256	13 × 13 × 256	3 × 3/1	Relu
	MaxPooling	256	6 × 6×256	3 × 3/2	Relu
6	FC	–	9216 × 1	–	Relu
7	FC	–	4096 × 1	–	Relu+Dropout
8	FC	–	4096 × 1	–	Relu+Dropout
	Output	–	3	–	Softmax

follows [50]:

$$p(\hat{y}_i = g\mathbf{I}_i) = \frac{\exp\left(\left(\boldsymbol{w}_g^{(2)}\right)^T h_i^{(1)}\right)}{\sum_{j=1}^{G}\exp\left(\left(\boldsymbol{w}_j^{(2)}\right)^T h_i^{(1)}\right)} \tag{13}$$

where $\boldsymbol{w}_g^{(2)} = \left[\boldsymbol{w}_1^{(2)}, \boldsymbol{w}_2^{(2)}, .., \boldsymbol{w}_G^{(2)}\right]$ are the weights of the softmax regression layer of dimension $D^{(1)\times G}$ and the superscript $(.)^T$ refers to the transpose operation. The learning process for all weights of network is performed using the back-propagation algorithm.

3. Results

The effectiveness of the proposed ECG diagnosis system is demonstrated by investigating 972 ECG segments taken from MIT-BIH ARR, MIT-BIH NSR, and BIDMC CHF databases. These databases are chosen based on the availability of the ECG signals belonging to the three classes under investigation: CHF, ARR, and NSR. The 972 ECG segments are composed of 576 ECG segments from 47 subjects diagnosed with ARR, 180 ECG segments from 15 subjects diagnosed with CHF, and 216 ECG segments from 18 NSR cases. Table 2 summarizes the ECG data distribution from both the MIT-BIH and BIDMC databases. As shown in Table 2, the ECG records used in this study consist of different cases of patient age and patient gender. To investigate the effectiveness of the proposed diagnosis system, several evaluation metrics, including Accuracy (***ACC***), Precision (***Pr***), Sensitivity (***Se***), Specificity (***SP***), and computational time are obtained. The ***ACC*** indicates the number of correctly classified test cases, the ***Pr*** measures the rate of true positive among the positive predictions, the ***Se*** is the true positive rate, and the ***SP*** is the true negative rate. Those four metrics are expressed as follows [51]:

$$\text{Sensitivity } (Se) = TP/(TP + FN) \tag{14}$$

$$\text{Specificity } (SP) = TN/(TN + FP) \tag{15}$$

$$\text{Precision (Pr)} = TP/(TP + FP) \tag{16}$$

$$\text{Accuracy } (ACC) = (TP + TN)/(TP + FP + TN + FN) \tag{17}$$

where *TP* is the true positive, *TN* is the true negative, *FP* is the false positive, and *FN* is the false negative.

Table 2
Categories of ECG records examined from the MIT-BIH and BIDMC databases.

ECG	Segments	Subjects	Subjects		Age (years)	
			Male	Female	Male	Female
ARR	576	47	25	22	32 to 89	23 to 89
CHF	180	15	11	4	22 to 71	54 to 63
NSR	216	18	5	13	26 to 45	20 to 50

Separate patients (records) are investigated in the training and testing as follows: 79 ARR, 24 CHF, and 30 NSR records are used for training and validation, yielding a total of 802 segments for the training stage, while 17 ARR, 6 CHF, and 6 NSR records are reserved exclusively for testing, forming a total of 170 segments for the testing stage. The training data is used to train the model, and the validation data is used to provide an unbiased evaluation of a model fit on the training dataset while tuning model hyperparameters. The test data has never been used in the training and it is utilized to provide an unbiased evaluation of the final model. To validate the classification results and reduce any possible deviation, the k-fold cross-validation technique is employed [41]. In the current study, the 5-fold cross-validation is employed, where the training and validation data (802 ECG segments from specific 79 ARR, 24 CHF, and 30 NSR records) are divided randomly into five groups with equal size, every time one group is chosen for validation and the other four groups are used for training. The test data (170 segments) are taken from the other remaining patients (17 ARR, 6 CHF, and 6 NSR records). The classification metrics (*ACC*, *Se*, *SP*, and *Pr*) are calculated for each fold corresponding to the test data of the three classes ARR, CHF, and NSR. The 5-fold average classification *ACC*, *Se*, *SP*, and *Pr* are computed by averaging the classification results of the 5-rounds for the test data of

Table 3
The 5-fold cross-validation classification results of the proposed approach (AlexNet with CQ-NSGT) using 972 ECG segments from the MIT-BIH and BIDMC databases.

Fold	Type	Performance parameter			
		Se %	*Sp* %	*Pr*[f_0] %	*Acc* %
Fold-1	**ARR**	97.09	100.00	100.00	98.24
	CHF	100.00	99.29	96.67	99.41
	NSR	100.00	98.48	95.00	98.82
Fold-2	**ARR**	98.04	100.00	100.00	98.82
	CHF	100.00	100.00	100.00	100.00
	NSR	100.00	98.48	95.00	98.82
Fold-3	**ARR**	97.06	98.53	99.00	97.65
	CHF	96.67	99.29	96.67	98.82
	NSR	100.00	98.48	95.00	98.82
Fold-4	**ARR**	96.15	100.00	100.00	97.65
	CHF	100.00	99.29	96.67	99.41
	NSR	100.00	97.74	92.50	98.24
Fold-5	**ARR**	98.04	100.00	100.00	98.82
	CHF	100.00	100.00	100.00	100.00
	NSR	100.00	98.48	95.00	98.82
Average	**ARR**	**97.28 ± 0.01**	**99.71 ± 0.01**	**99.80 ± 0.00**	**98.24 ± 0.01**
	CHF	**99.33 ± 0.01**	**99.57 ± 0.00**	**98.00 ± 0.02**	**99.53 ± 0.00**
	NSR	**100 ± 0.00**	**98.34 ± 0.00**	**99.8 ± 0.01**	**98.71 ± 0.00**
Overall performance		**98.87**	**99.21**	**99.20**	**98.82**

the three classes (ARR, CHF, and NSR) as shown in Table 3. Also, the standard deviation of 5-fold cross-validation results is calculated for each metric corresponding to the three classes ARR, CHF, and NSR (see Table 3). This method ensures the authentication and validity of all classification results in the current study.

Table 3 shows the 5-fold classification results for CHF, ARR, and NSR using the proposed diagnosis system (AlexNet with CQ-NSGT). Table 3 reveals that the proposed approach achieves superior performance in terms of average *Se* (97.28% for ARR, 99.33% for CHF, and 100% for NSR), *ACC* (98.24% for ARR, 99.53% for CHF, and 98.71% for NSR), *Pr* (99.80% for ARR, 98% for CHF, and 99.80% for NSR) and *SP* (99.71% for ARR, 99.57% for CHF, and 98.34% for NSR).

The training progress of the proposed approach is investigated to understand how quickly the network accuracy is improving, and whether the network is starting to overfit the training data. Fig. 5a shows the training accuracy and validation accuracy for the proposed approach (AlexNet with CQ-NSGT), revealing high validation accuracy of 96.25%. Note that in each iteration, an estimation of the loss function gradient is computed, and the network parameters are updated. As shown in Fig. 5, each training epoch is marked with shaded background.

3.1. Performance analysis

In order to evaluate the usefulness of the proposed CQ-NSGT algorithm, we compared its performance with the well-known CWT algorithm [52], while keeping the same techniques and parameters for other stages of the diagnosis system. Table 4 shows the 5-fold classification results for CHF, ARR, and NSR using the AlexNet architecture with CWT. In comparing Table 3 and 4, it can be noted that the proposed AlexNet with CQ-NSGT algorithm is superior over the AlexNet with CWT algorithm in terms of the diagnosis performance metrics for the three classes under investigation: CHF, ARR, and NSR. The training progress of the AlexNet architecture with CWT algorithm is compared with the proposed AlexNet with CQ-NSGT approach as shown in Fig. 5. In comparing Fig. 5a and b, it can be seen that the proposed AlexNet with CQ-NSGT technique has faster and better training progress than the AlexNet with CWT algorithm. Also, the proposed approach achieves higher performance than the AlexNet with CWT in terms of the validation accuracy (96.25% versus 90.32%).

Fig. 6 illustrates the average 5-fold classification *ACC*, *Se*, *SP*, and *Pr* for the three classes of CHF, ARR, and NSR using both the proposed AlexNet with CQ-NSGT algorithm and the AlexNet with CWT algorithm. As shown in Fig. 6, the CQ-NSGT algorithm is superior over the CWT algorithm in terms of the average classification *ACC* (98.82% versus

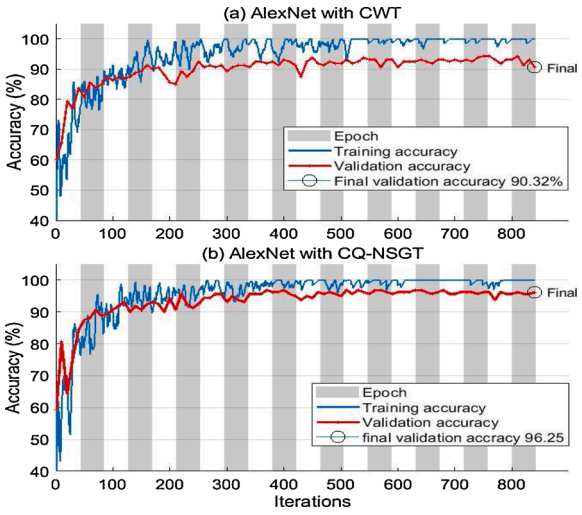

Fig. 5. Training and validation accuracy of the AlexNet architecture using (a) the proposed CQ-NSGT and (b) the CWT.

Table 4
The 5-fold cross-validation classification results of the AlexNet architecture with CWT using 972 ECG segments from the MIT-BIH and BIDMC databases.

Fold	Type	Performance parameter			
		Se %	*Sp* %	*Pr*[J0] %	*Acc* %
Fold-1	ARR	90.09	100.00	100	93.53
	CHF	100.00	97.22	86.67	97.65
	NSR	96.97	94.16	80.00	94.71
Fold-2	ARR	90.91	100.00	100.00	94.12
	CHF	100.00	97.90	90.00	98.24
	NSR	96.97	94.16	80.00	94.71
Fold-3	ARR	85.47	100.00	100.00	90.00
	CHF	100.00	97.22	86.67	97.65
	NSR	100.00	90.91	67.50	92.35
Fold-4	ARR	86.21	100.00	100.00	90.59
	CHF	100.00	97.90	90.00	98.24
	NSR	100.00	90.91	67.50	92.35
Fold-5	ARR	87.72	100.00	100.00	91.76
	CHF	100.00	96.55	83.33	97.06
	NSR	96.77	92.81	75.00	93.53
Average	**ARR**	**88.08 ± 0.02**	**100 ± 0.00**	**100 ± 0.00**	**92 ± 0.02**
	CHF	**100 ± 0.00**	**97.36 ± 0.01**	**87.33 ± 0.03**	**97.76 ± 0.00**
	NSR	**98.14 ± 0.02**	**92.59 ± 0.02**	**100 ± 0.06**	**93.53 ± 0.01**
Overall performance		**95.41**	**96.65**	**95.78**	**94.43**

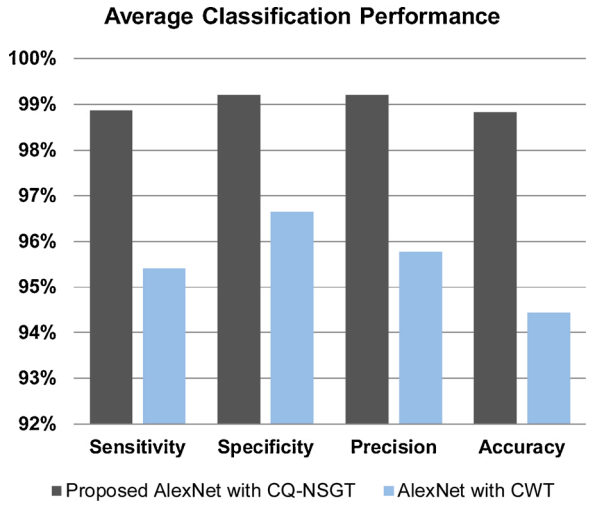

Fig. 6. The average 5-fold classification results of the proposed AlexNet with CQ-NSGT versus the AlexNet with CWT.

94.43%), *Se* (98.87% versus 95.41%), *SP* (99.21% versus 96.65%), and *Pr* (99.20% versus 95.78%). It can be also seen that the proposed CQ-NSGT algorithm is significantly more robust and efficient than the CWT, while the computational efficiency of both techniques is nearly the same. This reveals the effectiveness of the proposed AlexNet with CQ-NSGT algorithm in enhancing the diagnosis performance of CHF, ARR, and NSR over other existing systems.

The proposed ECG diagnosis approach is also compared with other recent techniques [11,12,14–17,32–35], and the results are shown in Table 5. The proposed system has the highest *ACC* of 98.82% using shorter ECG segments than

all other approaches. Table 5 reveals that the proposed approach achieves superior performance over other techniques [11,12,14–16,32, 34,35] in reducing the number of false negatives and consequently, providing the highest *Se* of 98.87%. Also,

the proposed technique has comparable sensitivity with the efficient

Table 5
Comparison between the proposed diagnosis system and other existing approaches.

Author Year	Physionet Data	Time scale	Method	Performance		
				Se	*Sp*	*Acc*
David et al. [11] 2016	MIT-BIH NSR db (18) BIDMC CHF db (15)	1000 RR intervals (13 min)	K-NN, Renyi entropy in addition to standard HRV time domain measures	80.0	94.4	87.9
Chen et al. [12] 2016	MIT-BIH NSR RR, NSR db (72), BIDMC CHF RR db (44)	Short term 5 min	4-level CHF detection and quantification using dynamic HRV measures and DT-SVM algorithm	95.39	100	96.91
Kumar et al. [14] 2017	MIT-BIH NSR db (18) BIDMC CHF db (15)	500 samples	FAWT, AFEnt, APEnt combined with LS-SVM	98.07	98.33	98.21
Wang et al. [15] 2018	MIT-BIH NSR RR db (52) BIDMC CHF RR db (18)	Short term 5 min	SVM with time domain, frequency domain, and nonlinear Sample Entropy	91.31	90.04	90.95
B. Hu et al. [16] 2019	MIT-BIH NSR RR db (54) BIDMC CHF RR db (29)	From 5 min to 10h	SVM with 7 different time scales HRV signals	93.33	98.33	94.44
Isler et al. [17] 2019	MIT-BIH NSR RR db (54) BIDMC CHF RR db (29)	Short term 5 min	3 stage classifier with time domain, frequency domain, and nonlinear SampEn, ApEn, DFA, Pointcare plot	100	98.1	98.80
Zhang et al. [32] 2018	MIT-BIH NSR RR db (54) BIDMC CHF RR db (29)	Short term 5 min	CNN with Distance distribution matrix	80.99	–	81.34
Kaouter et al. [33] 2019	MIT-BIH NSR db (18) BIDMC CHF db (15) MIT-BIH ARR db (48)	short term 8min	CNN with CWT	–	–	93.75
Acharya et al. [34] 2019	MIT-BIH NSR db (18) BIDMC CHF db (15)	short term 2 s	Automatically feature extraction with 11-layer DCNN	96.52	95.75	95.98
Wang et al. [35] 2019	MIT-BIH NSR RR db (54) BIDMC CHF RR db (29)	short term 500 sample	Expert features, DCNN with Ensemble classifier	76.71	99.22	87.54
Proposed Approach	**MIT-BIH NSR db (18) BIDMC CHF db (15) MIT-BIH ARR db (48)**	**Very Short segments 10,000 samples (1.3 min)**	**Automatically feature extraction with Pre-trained CNN, AlexNet and CQ-NSGT**	**98.87**	**99.21**	**98.82**

approach of [17], while achieving higher accuracy and specificity. It can be noted that the specificity of the proposed diagnosis system is higher than the techniques of [11,14–17,32], and is comparable with the diagnosis system of [12,35].

Note that most of recent studies distinguished only patients diagnosed with CHF from NSR [11,12,14–17,32,34,35], while the proposed approach provides ECG multiclass diagnosis by distinguishing not only patients diagnosed with CHF from NSR subjects but also from ARR subjects with overall average classification *ACC* of 98.82%, *Se* of 98.87%, and *SP* of 99.21%. Also, the proposed approach is employed directly on the input ECG data without the need of R-peak detection. Furthermore, the proposed approach requires shorter ECG segments (1.3 min) than studies under comparison [11,12,14–17,32,33,35]. This demonstrates the usefulness of the proposed approach in ECG multiclass diagnosis. Some studies under comparison employed simple classifiers trained on a set of hand-crafted features extracted from the HRV analysis [11,12,14–17]. The performance of such classifiers is mainly dependent on the feature selection process, which is difficult and time consuming, while requiring large amount of ECG data. The proposed approach overcomes the drawbacks of hand-crafted feature extraction and selection by leveraging a pre-trained CNN architecture, AlexNet, fed with time-frequency representations of the input ECG using the CQ-NSGT algorithm. Also, leveraging a pre-trained deep CNN avoids training of a deep NN from scratch.

4. Discussion and conclusions

In this paper, a new automated DL approach is proposed for ECG multiclass diagnosis of CHF, ARR, and NSR with high accuracy. The proposed ECG diagnosis system investigates the CQ-NSGT algorithm for transforming the input 1-D ECG signal into 2-D time-frequency representation which will be fed to the pre-trained AlexNet CNN architecture. To the authors' knowledge, it is the first time to combine the proposed CQ-NSGT algorithm with a pretrained CNN architecture in one fully automated diagnosis system that results in highly accurate ECG multiclass classification using low to medium hardware requirements. The effectiveness of the proposed diagnosis system is demonstrated by investigating several ECG records representing different cases of patient age and patient gender from the MIT-BIH and BIDMC databases. The performance of ECG classification for the three cardiac conditions CHF, ARR, and NSR is evaluated in terms of *ACC*, *Se*, *SP*, and *Pr*. The average classification results using 5-fold cross-validation are obtained in order to validate the results of the proposed system.

Experimental results reveal that the proposed approach achieves high diagnosis performance with overall average *ACC* of 98.82%, *Se* of 98.87%, *SP* of 99.21%, and *Pr* of 99.20%. The proposed approach is also compared with other recent diagnosis systems, and the results reveal the superior performance of the proposed system as shown in Table 5.

The AlexNET architecture is compared with other CNN deep models, including VGG-16, VGG-19, ResNet-50, ResNet-101, Inception-v3, and DenseNet, and the results are shown in Table 6. Results reveal that the AlexNET model outperforms other CNN architectures by achieving the highest classification results and taking the shortest processing time. The highest classification performance of AlexNet architecture over other deep models comes from the fact that the 2-D signal resulted from ECG transformation is a relatively simple image, so there is no need to have a depth layer in the CNN architecture. The use of deep layers leads to an increase in the free parameters, which can cause over-fitting and performance degradation. Note that for large-scale datasets such as ImageNet, deeper networks outperform shallow ones because the data is diverse, and the networks learn abstractions for a huge selection of classes. On contrast, in ECG classification, the data variability is several orders of magnitude smaller than image classification problems, and therefore deeper networks are not efficient for ECG classification. The AlexNet architecture has a faster convergence rate and better training performance than other deep CNN architectures. This reveals the high computational efficiency of the AlexNet architecture for ECG diagnosis systems.

The performance of the proposed approach is further investigated by evaluating the CQ-NSGT algorithm used in ECG-to-image transformation and comparing its performance with the CWT algorithm. As shown in Fig. 5, the proposed AlexNet with CQ-NSGT technique has faster and better training progress than the AlexNet with CWT algorithm. Also, the proposed AlexNet with CQ-NSGT approach outperforms the AlexNet with CWT in terms of the validation accuracy (96.25% versus 90.32%). It can be noted from Tables 3 and 4 that the proposed system is superior over the AlexNet with CWT algorithm in terms of the diagnosis performance metrics for the three cardiac conditions CHF, ARR, and NSR. The overall computational time of the proposed diagnosis system using MATLAB software is around 2.9 h for training and 61.49 s for testing on a personal laptop with the following specifications: Intel core i7-4600 M CPU, 2.9 GHz, 8 GB RAM, and 64-bit windows 10

Table 6
Comparison between the AlexNet model and other CNN architectures.

Metric	AlexNET	VGG-16	VGG-19	ResNet-50	ResNet-101	Inception-v3	DenseNet
Se %	**98.87**	97.63	98.12	94.93	96.54	94.67	95.57
Sp %	**99.21**	98.71	96.42	96.67	96.56	95.34	96.32
$Pr[f_0]$ %	**99.20**	98.10	95.30	95.49	97.53	95.13	95.40
Acc %	**98.82**	97.64	95.55	95.79	96.37	96.12	96.32

operating system. This reveals the effectiveness of the proposed system in improving the accuracy of ECG multiclass diagnosis systems with low computational requirements.

CRediT authorship contribution statement

Ahmed S. Eltrass: Writing - review & editing, Investigation, Validation. **Mazhar B. Tayel:** Supervision. **Abeer I. Ammar:** Conceptualization, Methodology, Software, Data curation.

Declaration of Competing Interest

The authors declare that they have no known competing financial interests or personal relationships that could have appeared to influence the work reported in this paper.

References

[1] P. Ponikowski, A.A. Voors, S.D. Anker, H. Bueno, J.G. Cleland, A.J. Coats, V. Falk, J.R. González-Juanatey, V.P. Harjola, E.A. Jankowska, M. Jessup, ESC Guidelines for the diagnosis and treatment of acute and chronic heart failure: the Task Force for the diagnosis and treatment of acute and chronic heart failure of the European Society of Cardiology (ESC). Developed with the special contribution of the Heart Failure Association (HFA) of the ESC, Eur. J. Heart Fail. 18 (8) (2016) 891–975.

[2] M. Faezipour, A. Saeed, S.C. Bulusu, M. Nourani, L. Minn, A patient adaptive profiling scheme for ECG beat classification, IEEE Trans. Inf. Technol. 14 (5) (2010) 1153–1165.

[3] T. Kishi, Heart failure as an autonomic nervous system dysfunction, J. Cardiol. 59 (2) (2012) 117–122.

[4] G. Engström, B. Hedblad, S. Juul-Möller, P. Tydén, L. Janzon, Cardiac arrhythmias and stroke: increasedrisk in men with high frequency of atrial ectopic beats, Stroke 31 (12) (2000) 2925–2929.

[5] I. Lee, D. Kim, S. Kang, S. Lee, Ensemble deep learning for skeleton based action recognition using temporal sliding LSTM networks, in: Proceedings of the IEEE International Conference on Computer Vision, Venice, Italy, 2017, pp. 1012–1020.

[6] Y. LeCun, Y. Bengio, G. Hinton, Deep learning, Nature 521 (7553) (2015) 436–444.

[7] G.E. Hinton, S. Osindero, Y.W. Teh, A fast learning algorithm for deep belief nets, Neural Comput. 18 (7) (2006) 1527–1554.

[8] J. Schmidhuber, Deep learning in neural networks: an overview, Neural Network. 61 (2015) 85–117.

[9] L. Pecchia, P. Melillo, M. Sansone, M. Bracale, Discrimination power of short-term heart rate variability measures for CHF assessment, IEEE Trans. Inf. Technol. Biomed. 15 (1) (2010) 40–46.

[10] G. Liu, L. Wang, Q. Wang, G. Zhou, Y. Wang, Q. Jiang, A new approach to detect congestive heart failure using short-term heart rate variability measures, PLoS One 9 (4) (2014) e93399.

[11] D.J. Cornforth, H.F. Jelinek, Detection of congestive heart failure using Renyi entropy, in: Vancouver, CanadaIEEE Computing in Cardiology Conference (CinC), vol. 43, 2016, pp. 669–672.

[12] W. Chen, L. Zheng, K. Li, Q. Wang, G. Liu, Q. Jiang, A novel and effective method for congestive heart failure detection and quantification using dynamic heart rate variability measurement, PLoS One 11 (11) (2016) e0165304.

[13] Z. Masetic, A. Subasi, Congestive heart failure detection using random forest classifier, Comput. Methods Programs Biomed. 130 (2016) 54–64.

[14] M. Kumar, R.B. Pachori, U.R. Acharya, Use of accumulated entropies for automated detection of congestive heart failure in flexible analytic wavelet transform framework based on short-term HRV signals, Entropy 19 (3) (2017) 92.

[15] Y. Wang, S. Wei, S. Zhang, Y. Zhang, L. Zhao, C. Liu, A. Murray, Comparison of time-domain, frequency-domain and non-linear analysis for distinguishing congestive heart failure patients from normal sinus rhythm subjects, Biomed. Signal Process. Control 42 (2018) 30–36.

[16] B. Hu, S. Wei, D. Wei, L. Zhao, G. Zhu, C. Liu, Multiple time scales analysis for identifying congestive heart failure based on heart rate variability, IEEE Access 7 (2019) 17862–17871.

[17] Y. Isler, A. Narin, M. Ozer, M. Perc, Multi-stage classification of congestive heart failure based on short-term heart rate variability, Chaos Solitons Fractals 118 (1) (2019) 145–151.

[18] C. Potes, S. Parvaneh, A. Rahman, B. Conroy, Ensemble of featurebased and deep learning-based classifiers for detection of abnormal heart sounds, in: IEEE Computing in Cardiology Conference (CinC), Vancouver, Canada, 2016, pp. 621–624.

[19] B. Hwang, J. You, T. Vaessen, I. Myin-Germeys, C. Park, B.T. Zhang, Deep ECGNet: an optimal deep learning framework for monitoring mental stress using ultra short-term ECG signals, Telemed. E-health 24 (10) (2018) 753–772.

[20] B. Pourbabaee, M.J. Roshtkhari, K. Khorasani, Deep convolutional neural networks and learning ECG features for screening paroxysmal atrial fibrillation patients, IEEE Trans. Syst. Man Cybern. Syst. 48 (12) (2018) 2095–2104.

[21] W. Chen, G. Liu, S. Su, Q. Jiang, H. Nguyen, A CHF detection method based on deep learning with RR intervals, in: The 39th Annual International Conference of the IEEE Engineering in Medicine and Biology Society (EMBC), Jeju Island, Korea, 2017, pp. 3369–3372.

[22] G. Altan, Diagnosis of coronary artery disease using deep belief networks, Eur. J. Eng. Nat. Sci. 2 (1) (2017) 29–36.

[23] N. Tajbakhsh, J.Y. Shin, S.R. Gurudu, R.T. Hurst, C.B. Kendall, M.B. Gotway, J. Liang, Convolutional neural networks for medical image analysis: full training or fine tuning? IEEE Trans. Med. Imaging 35 (5) (2017) 1299–1312.

[24] H. Azizpour, A.S. Razavian, J. Sullivan, A. Maki, S. Carlsson, Factors of transferability for a generic ConvNet representation, IEEE Trans. Pattern Anal. Mach. Intell. 38 (9) (2015) 1790–1802.

[25] A. Krizhevsky, I. Sutskever, G.E. Hinton, ImageNet classifcation with deep convolutional neural networks, Adv. Neural Inf. Process. Syst. 25 (2) (2012) 1097–1105.

[26] K. Simonyan, A. Zisserman, Very deep convolutional networks for large-scale image recognition, arXiv preprint arXiv:1409 1556 (2014).

[27] C. Szegedy, W. Liu, Y. Jia, P. Sermanet, S. Reed, D. Anguelov, D. Erhan, V. Vanhoucke, A. Rabinovich, Going deeper with convolutions, in: The 28th IEEE Conference on Computer Vision and Pattern Recognition (CVPR), Boston, Massachusetts, USA, 2015, pp. 1–9.

[28] A. Kumar, J. Kim, D. Lyndon, M. Fulham, D. Feng, An ensemble of fine-tuned convolutional neural networks for medical image classification, IEEE J. Biomed. Health Inform. 21 (1) (2016) 31–40.

[29] Y. Yu, H. Lin, J. Meng, X. Wei, H. Guo, Z. Zhaio, Deep transfer learning for modality classification of medical images, Information 8 (3) (2017) 91.

[30] U.K. Lopes, J.F. Valiati, Pre-trained convolutional neural networks as feature extractors for tuberculosis detection", Comput. Biol. Med. 89 (2017) 135–143.

[31] V.J.R. Ribas, A. Wojdel, E. Romero, P. Ramos, J. Brugada, ECG assessment based on neural networks with pretraining, Appl. Soft Comput. 49 (2016) 399–406.

[32] Y. Li, Y. Zhang, L. Zhao, Y. Zhang, C. Liu, L. Zhang, Z. Li, B. Wang, E. Ng, J. Li, Combining convolutional neural network and distance distribution matrix for identification of congestive heart failure, IEEE Access 6 (2018) 39734–39744.

[33] K. Kaouter, T. Mohamed, D. Sofiene, D. Abbas, M. Fouad, Full training convolutional neural network for ECG signals classification, in: AIP Conference Proceedings (Vol. 2190, No. 1, p. 020055), AIP Publishing LLC, Athens, Greece, 2019.

[34] U.R. Acharya, H. Fujita, S.L. Oh, Y. Hagiwara, J.H. Tan, M. Adam, R. San Tan, Deep convolutional neural network for the automated diagnosis of congestive heart failure using ECG signals, Appl. Intell. 49 (1) (2019) 16–27.

[35] L. Wang, W. Zhou, Q. Chang, J. Chen, X. Zhou, Deep ensemble detection of congestive heart failure using short-term RR intervals, IEEE Access 7 (2019) 69559–69574.

[36] A.L. Goldberger, L.A. Amaral, L. Glass, J.M. Hausdorff, P.C. Ivanov, R.G. Mark, J. E. Mietus, G.B. Moody, C.K. Peng, H.E. Stanley, Physiobank, physiotoolkit, and physionet: components of a new research resource for complex physiologic signals, Circulation 101 (23) (2000) e215–e220.

[37] G.B. Moody, R.G. Mark, The impact of the MIT-BIH arrhythmia database, IEEE Eng. Med. Biol. Mag. 20 (3) (2001) 45–50.

[38] D.S. Baim, W.S. Colucci, E.S. Monrad, H.S. Smith, R.F. Wright, A. Lanoue, Survival of patients with severe congestive heart failure treated with oral milrinone, J. Am. Coll. Cardiol. 7 (3) (1986) 661–670.

[39] N. Ghanem, A.S. Eltrass, N.H. Ismail, Investigation of EEG noise and artifact removal by patch-based and kernel adaptive filtering techniques, in: The 13th Annual IEEE International Symposium on Medical Measurements and Applications (MeMeA), Rome, Italy, 2018.

[40] M.B. Tayel, A.S. Eltrass, A.I. Ammar, A new multi stage combined kernel filtering approach for ECG noise removal, J. Electrocardiol. 51 (2) (2018) 265–275.

[41] M. Stone, Cross-validatory choice and assessment of statistical predictions, J. R. Stat. Soc. Ser. B 36 (2) (1974) 111–133.

[42] M. Yochum, C. Renaud, S. Jacquir, Automatic detection of P, QRS and T patterns in 12 leads ECG signal based on CWT, Biomed. Signal Process. Control 25 (2016) 46–52.

[43] R.S. Remya, K.P. Indiradevi, K.A. Babu, Classification of myocardial infarction using multi resolution wavelet analysis of ECG, Procedia Technol. 24 (5) (2016) 949–956.
[44] V. Nannaparaju, S. Narasimman, Detection of T-wave alternans in ECGs by wavelet analysis, Procedia Mater. Sci. 10 (2015) 307–313.
[45] M. Thomas, M.K. Das, S. Ari, Automatic ECG arrhythmia classification using dual tree complex wavelet based features, AEU—Int. J. Electron. Commun. 69 (4) (2015) 715–721.
[46] J.C. Brown, Calculation of a constant Q spectral transform, J. Acoust. Soc. Am. 89 (1) (1991) 425–434.
[47] G.A. Velasco, N. Holighaus, M. Dörfler, T. Grill, Constructing an invertible constant-Q transform with non stationary Gabor frames, in: The 14th International Conference on Digital Audio Effects, Paris, France, 2011, pp. 93–99.
[48] N. Holighous, M. Dorfler, G.A. Velasco, T. Grill, A framework for invertible, real-time constant-Q transforms, IEEE Trans. Audio Speech Lang. Process. 21 (4) (2012).
[49] H.G. Feichtinger, T. Strohmer, Advances in Gabor Analysis, Springer Science & Business Media, USA, 2012.
[50] M.M. Al Rahhal, Y. Bazi, M. Al Zuair, E. Othman, B. BenJdira, Convolutional neural networks for electrocardiogram classification, J. Med. Biol. Eng. 38 (6) (2018) 1014–1025.
[51] R. Duda, E. Hart, D. Stork, Pattern Classification, John Wiley & Sons, NY, USA, 2000.
[52] C. Saritha, V. Sukanya, Y.N. Murthy, ECG signal analysis using wavelet transforms, Bulg. J. Phys 35 (no. 1) (2008) 68–77.